AN ELECTRODELESS DRIFT CHAMBER OF MEDIUM SIZE CELL

George S. Tzanakos
Columbia University, New York, NY 10027

Summary

An electrodeless drift chamber of medium size cell has been constructed and tested. Preliminary results with cosmics as well as with a radioactive source are presented.

Introduction

Several experiments in high energy physics require very large detectors with tracking and calorimetric capabilities. In order to reduce the cost of electronics, one has sometimes to use drift chambers with a large drift space. Since the aspect ratio (= maximum drift distance/drift gap) in such chamber is large, one needs to shape the drift field in order to make the chamber efficient. The field shaping is done with field shaping wires or with conducting strips, connected to an external resistor chain (Fig. 1a).

Chamber Design and Operation

A typical electrodeless drift chamber is shown schematically in Fig. 1b. A thin anode wire is held at positive potential between two grounded cathodes. The sides of the chamber that support the anode wire are made of plastic material. The structure is completed with a high quality insulator,[5] (G-10, for example), the outer side of which is copper-plated and held at the same potential as the cathodes. The function of this outer conductor is two-fold: (1) It establishes the field in the dielectric, which is necessary for the operation of the chamber; (2) it acts as a Faraday cage protecting the chamber from external noise.

When the chamber is first switched on, most of the field lines terminate on the outer conductor through the dielectric,

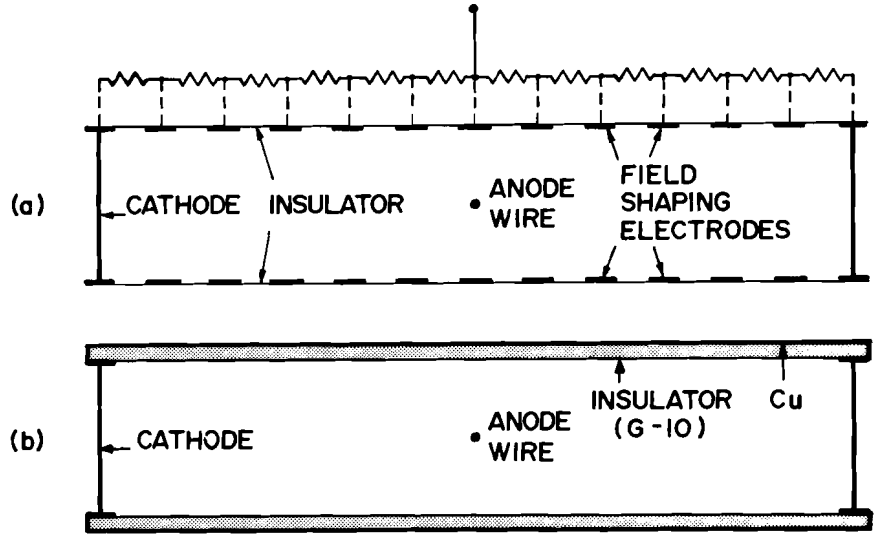

Fig. 1 (a) Schematic of a typical drift chamber cell with field shaping electrodes. The bottom electrodes are connected to the same resistive network. Three different power supplies are needed for the anode, cathodes, and the resistive network.
(b) Electrodeless drift chamber cell. Essential components are: anode, cathodes, and the single-sided copper-plated G-10 plates.

The electrodeless drift chamber is a much simpler device that needs neither field shaping electrodes nor the associated external resistor chain. The field shaping is done by positive charges deposited on dielectric surfaces. The first electrodeless chamber was constructed and tested by Allison et al.[1] Subsequently, several other groups[2-4] have constructed and tested electrodeless drift chambers of various cell configurations and sizes.

as shown in Fig. 2a. In the presence of ionizing radiation, the field configuration changes rapidly as positive ions, released near the anode (gain $\simeq 10^5$-10^6), follow the field lines and deposit their charge on the dielectric surfaces. This distribution of positive charges plays a role similar to that of field shaping electrodes. The steady state field configuration is shown in Fig.2b. The field lines terminate now on the cathodes. The field near the wire is radial, becoming uniform over most of the cell volume. This is a self-sustained state of dynamical equilibrium, where the positive charges,

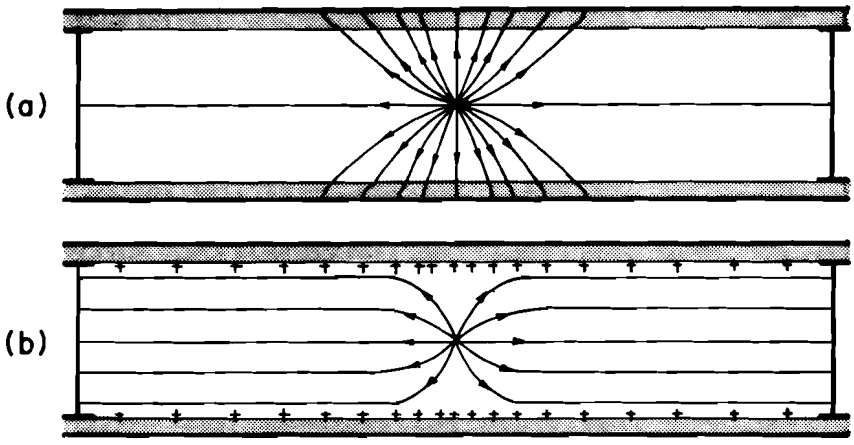

Fig. 2 Electric field configurations for an electrodeless drift chamber . (a) Field lines when the high voltage is first switched on. (b) Field lines at steady state.

leaking slowly through the dielectric to the outer conductor, as well as to the cathodes, are replaced with new charges deposited by positive ions reaching the inner surface of the dielectric.

The chamber parameters must be carefully optimized in the design. The drift velocity depends on the electric field, which, over most of the volume of the chamber, is determined by the high voltage and the maximum drift distance. The gas amplification, on the other hand, depends on the electric field near the wire which is determined by the wire diameter, the drift gap, and the high voltage. The loss of primary electrons in the chamber walls due to transverse diffusion must be taken into consideration in choosing the drift gap size. In addition, the purity of the gas mixture must be such as to minimize the loss of drifting electrons due to their attachment to electronegative agents.

The Prototype Chamber

A prototype chamber was built, by using 1/16 in. thick single-sided copper plated G-10 plates. The chamber parameters are: drift gap = 3/8 in., maximum drift distance = 2.25 in., length = 30 in. The anode was made of 30 μm gold plated tungsten wire. Aluminum I-beams were used as cathodes.

The signal processing electronics, designed by W. Sippach, is shown schematically in Fig. 3. The chamber signal, after amplification, is received differentially at the input of a 6-bit flash ADC system which samples and digitizes the pulse at 33 ns intervals. The digitized information is clocked into a 6-bit 256-word memory, which is read out to a computer, whenever a (delayed) event trigger is received. In this way, one has available in digital form all the pulse information for the last (256 x 33) ns ≃ 8.5 μs.

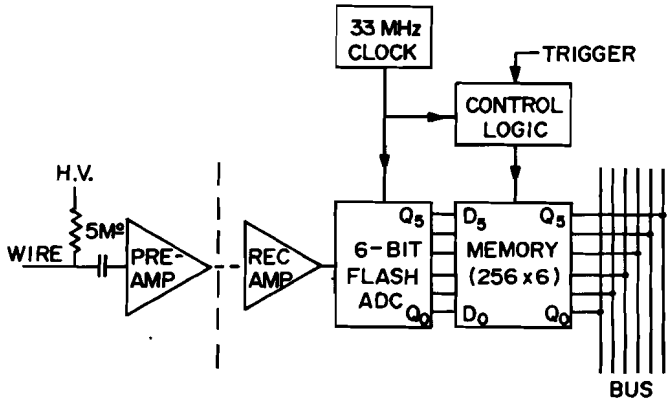

Fig. 3 Schematic of the signal processing electronics. The signal after amplification is received differentially (not shown) at the input of the 6-bit flash ADC. The trigger signal inhibits memory writing and initiates readout.

Chamber Performance

The chamber was installed in a cosmic ray scintillation counter telescope, shown schematically in Fig. 4, and it was operated with a gas mixture of argon-ethane in the ratio 70/30, with a high voltage of 4.5 kV on the anode wire. The triple coincidence $S_1 \cdot S_2 \cdot S_3$ of the telescope counters was used as a trigger for the flash ADC system. The cosmic ray flux through the chamber, as defined by the telescope, is uniform. Figure 5 shows a typical chamber pulse after digitization. The drift time, as well as the pulse height (pulse area), are trivial to extract from the digitized information.

Figure 6 shows the drift time distribution corresponding to a uniform flux of cosmic rays as defined by the telescope. The data were collected over a 48-hour period. The deviation from a uniform distribution can be understood in terms of the electric field dependence of the drift velocity and the geometry of the chamber. The ratio of

the number of the chamber hits to the total number of triggers is 0.386 ± 0.003, whereas the number expected from the geometry of the system is 0.375. This is consistent with an average efficiency of about 100%.

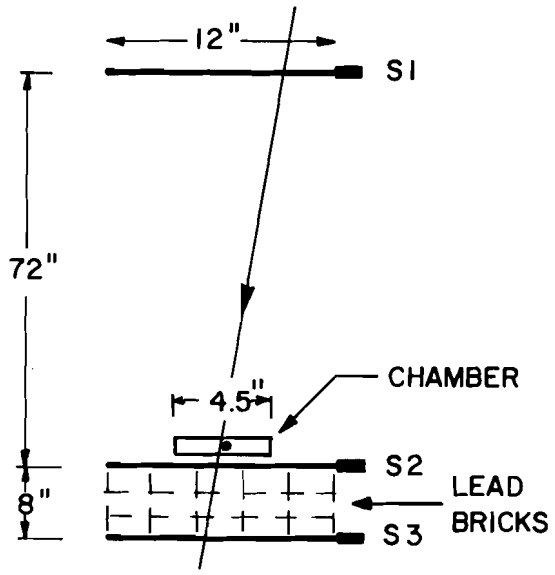

Fig. 4 The cosmic ray scintillation counter telescope (not to scale) and the approximate position of the chamber.

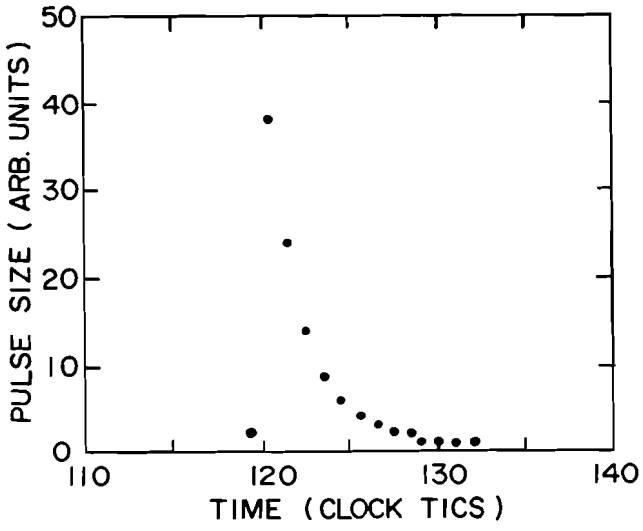

Fig. 5 A typical drift chamber pulse after amplification and digitization. Each clock tick represents 33 ns.

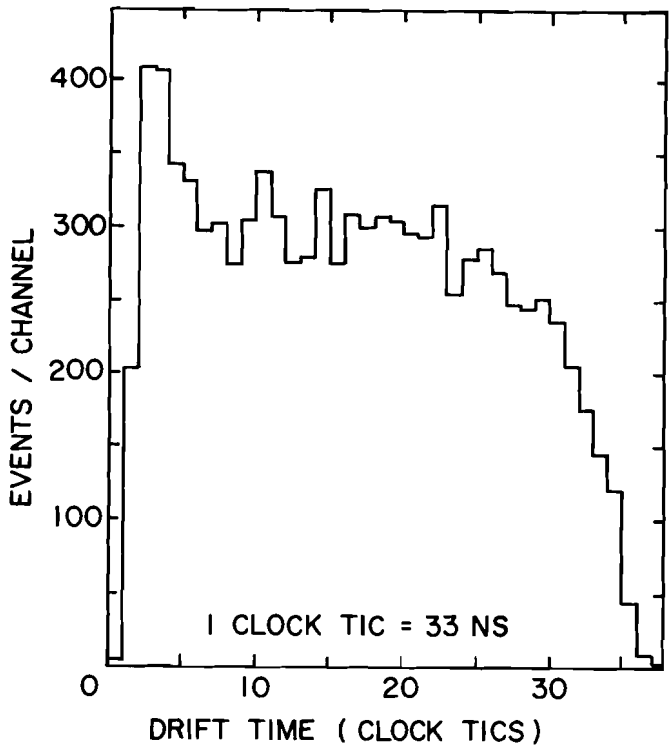

Fig. 6 Drift time distribution for a uniform flux of cosmic rays (see text). The maximum drift time (≃ 1.12 μs) corresponds to a maximum drift distance of 5.71 cm.

The pulse height distribution (Fig. 7) has the typical shape with the characteristic Landau tail. The dependence of the pulse height on the distance from the wire is shown in Fig. 8, where the mean pulse height is plotted against drift time. The plot shows almost no dependence on drift time, with the exception of the last point (furthestmost 3-5 mm), where the I-shaped cathode can distort the field configuration.

The performance of the chamber as a function of time for a few days of operation is shown in Fig. 9, where the average pulse height is plotted against real time. Each point represents the average pulse height for a period of 24 hours. The data show an attenuation of pulse height as a function of time. Such an attenuation has been observed elsewhere.[2] It has been interpreted as due to overcharging of the dielectric surfaces by positive ions diffused into the chamber walls on their way to the cathode. The evolution of the chamber performance over long periods of time is currently under investigation.

In addition to the above measurements, some qualitative observations have been made.

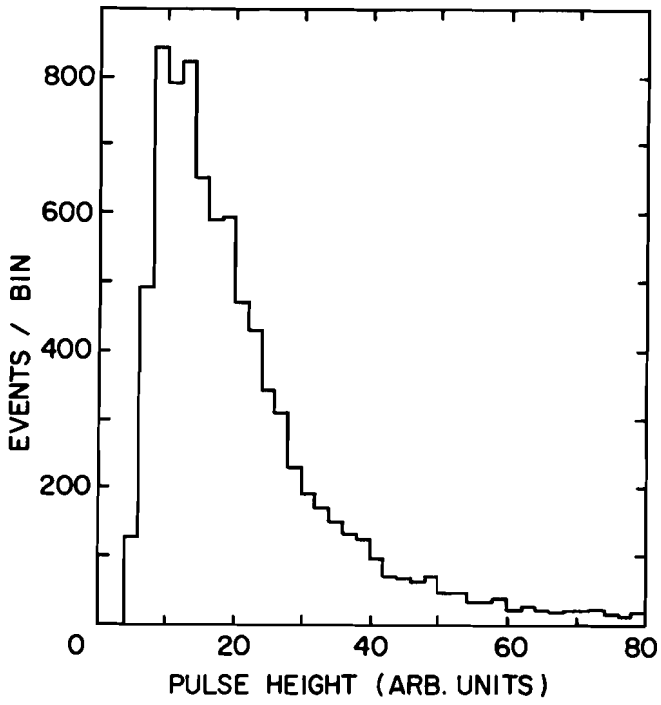

Fig. 7 Pulse height distribution of cosmic ray muons.

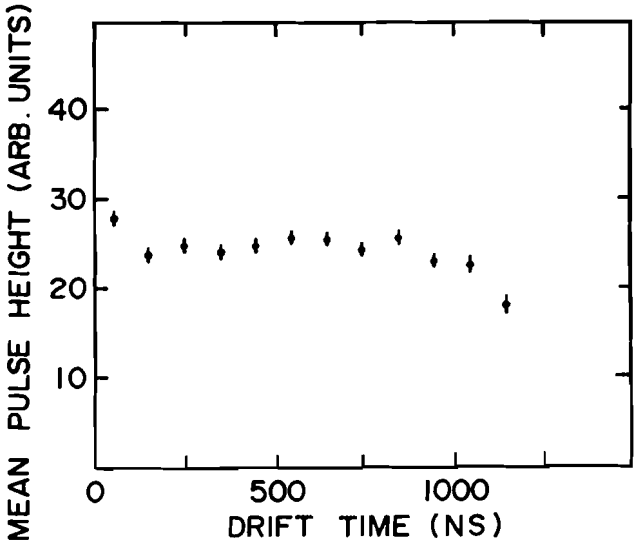

Fig. 8 Mean pulse height as a function of drift time.

a. The dielectric surfaces are charging up and the chamber becomes operational within minutes after the high voltage has been turned on.

b. After the dielectric has been charged up, a reduction of the high voltage by 50-100 volts is enough to kill the chamber signal. This hysteresis effect has been observed by Allison et al[1] also.

c. The use of a radioactive source (~ 10 kHz) has a dramatic effect on the chamber behavior: the signal amplitude is progressively diminished and the chamber becomes locally insensitive within minutes.

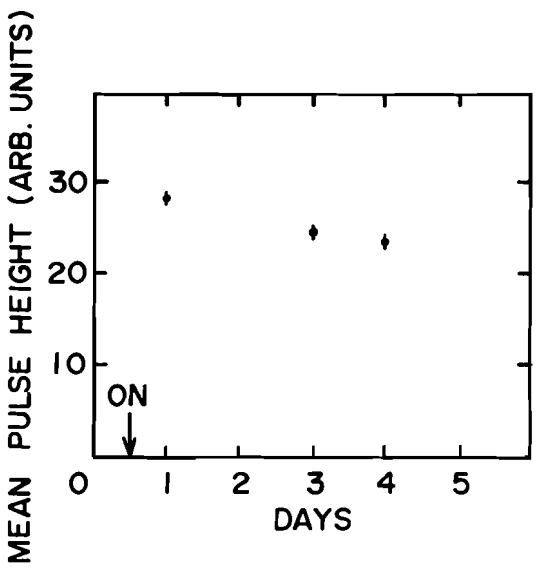

Fig. 9 Mean pulse height as a function of real time. An attenuation of the pulse height is visible.

In summary, an electrodeless drift chamber of medium cell size (maximum drift distance ≃ 6 cm, drift gap ≃ 1 cm) has been built and tested. Preliminary measurements with cosmic rays show a normal drift chamber behavior so far as drift time, pulse height, and efficiency are concerned. There are, however, serious questions concerning the chamber performance over long periods of time, as well as the maximum particle flux that it can take before starting deteriorating. These questions are currently under investigation.

I would like to thank Professor Frank Sciulli for bringing Ref. 1 to my attention and for many useful discussions. I would also like to thank W. Sippach for providing the electronics.

1. J. Allison, C.K. Bowdery, P.G. Rowe, "An Electrodeless Drift Chamber", U of Manchester preprint, MC 81/33 (Exp), 1981; submitted to NIM.
2. D. Ayres, L. Price, "Electrodeless Drift Chambers with 50-cm Drift Distance", contribution to this conference.
3. S. Errede, U of Michigan, private communication.
4. L. Pondrom, U of Wisconsin, priv. comm.
5. Typical values of volume resistivity and dielectric constant for G-10 are 5×10^{14} Ω·cm, and 5, respectively.